A Simple Method for Incorporating Madelung Field Effects into ab Initio Embedded Cluster Calculations of Crystals and Macromolecules

Eugene V. Stefanovich and Thanh N. Truong*

Henry Eyring Center for Theoretical Chemistry, Department of Chemistry, University of Utah, Salt Lake City, Utah 84112

Received: November 19, 1997; In Final Form: February 16, 1998

A new methodology is proposed for accurate and effective incorporation of the matrix elements of the Madelung potential into ab initio embedded cluster calculations of macromolecules, polar crystals, and their surfaces. The electrostatic potential from the infinite crystal lattice is modeled by a finite number (usually several hundred) of point charges located on a surface enclosing the cluster. A special boundary condition and the boundary element method are used to determine positions and magnitudes of these point charges. The advantages and accuracy of this approach are demonstrated on examples of water adsorption on the NaCl-(001) surface and the electrostatic field in a zeolite pore.

1. Introduction

In recent years the emphasis in theoretical chemistry has been shifting from properties of gas-phase molecules and reactions toward challenging areas of condensed-phase systems. Understanding physical and chemical processes in biopolymers, crystals, and solutions and at their interfaces is of great importance for further progress in medicine, technology, and environmental research. Embedded cluster calculations[1−3] of chemical processes in the condensed phase recently gained significant popularity due to their relatively low computational cost, flexibility, and reasonable accuracy. In embedded cluster quantum mechanical calculations of crystalline solids, one usually treats quantum mechanically only a small part of the crystal lattice. In what follows, we will refer to this quantum mechanical region as the *cluster*. The rest of the crystal will be called the *environment*. The action of the environment on electrons in the cluster is represented by an embedding potential $V_{\mathrm{embd}}(\mathbf{r})$. The embedding potential can be generated by many different approaches including the Green function technique,[4] density functional methods,[5] pseudopotential theory,[6−8] and other considerations. In LCAO-based methods, one needs analytical expressions for matrix elements $\langle\mu|V_{\mathrm{embd}}(\mathbf{r})|\nu\rangle$ of the embedding potential calculated over basis functions in the cluster. For many crystals of practical interest, the electrostatic, or Madelung, potential $V_{\mathrm{el}}(\mathbf{r})$ makes a dominant contribution to the total embedding potential. Many accurate techniques have been developed for calculating the Madelung potential $V_{\mathrm{el}}(\mathbf{r})$ at any given *point* in the bulk and near crystal surfaces. Perhaps, the best known is the Ewald summation method. However, an accurate calculation of the *matrix elements* of the Madelung potential $\langle\mu|V_{\mathrm{el}}(\mathbf{r})|\nu\rangle$ is not a trivial task.[9,10] Our goal in this study is to suggest a simple and yet accurate method for calculating the matrix elements of the Madelung potential assuming that the crystal potential at any given point can be found without difficulty, e.g., by using the Ewald technique.

Currently, there are basically two ways to deal with this Coulomb problem in ab initio calculations. The first approach involves a direct summation of the matrix elements of the Ewald potential given by analytical formulas derived by Saunders and his coauthors.[11] Due to the fast convergence of the Ewald-type series, the accuracy of such calculations can be systematically improved by increasing ranges of summation over both direct and reciprocal lattices. Although this approach, in principle, provides an ultimate and accurate solution for the electrostatic embedding potential, its implementation in existing molecular quantum chemistry programs requires significant efforts. To our knowledge, the total energy derivatives have not yet been implemented with this embedding method. For these reasons, in most practical calculations in the bulk and on the surface of crystals, another embedded cluster approach has been used thus far. In this common methodology, the infinite lattice potential is modeled by a finite number of point charges placed outside the cluster. Such an approach is attractive because analytical matrix elements of the point-charge potential, and often their first and second derivatives, are readily available in most quantum chemistry programs (nuclear attraction integrals). However, the accuracy of such a method critically depends on the selection of the total number of point charges, their positions $\mathbf{R}_i$, and values q_i. In most previous embedded cluster studies (for some recent applications see refs 12−15), these point charges were simply placed at ideal lattice sites and were assigned values corresponding to ionic charges in the crystal. In slightly more sophisticated methods, positions and/or values of peripheral point charges can be adjusted for better accuracy (see, e.g., references cited in ref 11). A well-known difficulty of such models is that results converge very slowly, if at all, when the size of the explicitly considered lattice is increased. Thus, there is no simple way for systematic improvement of results. Moreover, construction of such finite lattice models becomes more difficult for complex low-symmetry systems, such as proteins, zeolites,[16] and crystal surfaces.

So far, there is no universal prescription for how to select positions and values for a finite set of point charges to achieve the best possible representation of the potential generated inside the cluster by an infinite, or very large, point-charge lattice. In section 2 we suggest a simple procedure that can overcome this problem. For brevity, we call this formalism the SCREEP (surface charge representation of the electrostatic embedding potential) method. This method employs the conductor bound-

S1089-5647(98)00258-2 CCC: $15.00
Published on Web 03/31/1998

ary condition as a mathematical device to replace the Ewald summation of matrix elements. The same boundary condition has been suggested earlier by Klamt and Schüürmann in their COSMO solvation model[17] to approximate solvent polarization. It is important to note that although both methods use similar mathematical techniques, they apply to completely different physical models. The COSMO methodology approximates *polarization* of a polar liquid as if it were an ideal conductor. The use of the conductor boundary condition in the SCREEP model does not mean that any part of the system has conducting properties. This is merely a convenient mathematical tool designed to simplify calculations of matrix elements of the *electrostatic potential* in crystal or macromolecules. In section 3 we present applications of SCREEP to adsorption of water on the NaCl(001) surface and to the electrostatic potential in a zeolite pore. In particular, we discuss some parameters of the SCREEP method and how to achieve optimal accuracy at a reasonable computational cost.

2. The Surface Charge Representation of the Electrostatic Embedding Potential (SCREEP) Method

Consider a region of space C where the charge density is zero and the electrostatic potential in this region is produced by the charge distribution $\rho(\mathbf{r})$ lying entirely outside C. In the SCREEP model, C is the region occupied by cluster atoms, and $\rho(\mathbf{r})$ is the charge density in the environment. A well-known theorem from electrostatics states that no matter what is the charge distribution $\rho(\mathbf{r})$ *outside* C, its electrostatic potential $V_{el}(\mathbf{r})$ *inside* C can be rigorously replaced by some surface charge density $\sigma(\mathbf{r})$ located on the *boundary* S of the volume C. The demonstration goes as follows. First assume that we have filled the volume C with an ideal grounded metallic conductor. Then the electrostatic potential inside C becomes exactly zero independent of the external potential $V_{el}(\mathbf{r})$. Physically, this condition is satisfied due to creation of the charge density $-\sigma(\mathbf{r})$ on the surface S whose potential $-\oint_S \sigma(\mathbf{r}')/|\mathbf{r} - \mathbf{r}'|\, d^2r$ exactly compensates the external potential $V_{el}(\mathbf{r})$ for all points $\mathbf{r}$ on the surface S and in its interior.

$$V_{el}(\mathbf{r}) - \oint_S \frac{\sigma(\mathbf{r}')}{|\mathbf{r} - \mathbf{r}'|}\, d^2r = 0 \qquad (1)$$

Then, according to eq 1, the electrostatic potential generated by the charge density $\sigma(\mathbf{r})$ on the surface S and in its interior is exactly equal to the original potential $V_{el}(\mathbf{r})$. Note that the potential generated by $\sigma(\mathbf{r})$ *outside* the surface S is generally different from $V_{el}(\mathbf{r})$.

The option to rigorously substitute $\rho(\mathbf{r})$ by a charge density $\sigma(\mathbf{r})$ localized on a finite closed surface is important because often the charge distribution $\rho(\mathbf{r})$ may have a very complicated character (very large or even infinite number of atoms in biomolecules and crystals) which is not well suited for quantum calculations, e.g., calculations of matrix elements of the potential $V_{el}(\mathbf{r})$. For computational reasons, we resort to the boundary element method to represent the continuous surface charge density $\sigma(\mathbf{r})$. In this method, the surface S is divided into M surface elements with areas S_j. The surface charge density is now represented by a set of M point charges q_j located at the centers of surface elements $\mathbf{r}_j$

$$q_j \approx \sigma(\mathbf{r}_j) S_j \qquad (2)$$

This approximation is accurate when the surface S and the charge distribution $\sigma(\mathbf{r})$ are sufficiently smooth and the number of surface points M is large enough. Then eq 1 can be approximated by a matrix equation

$$V - \mathbf{A}q = 0 \qquad (3)$$

from which the vector of surface charges $\mathbf{q}$ can be determined by applying any common technique available for solving systems of linear equations. For example, one can use the matrix inversion method

$$q = \mathbf{A}^{-1}V \qquad (4)$$

In eqs 3 and 4, the vector V contains values of the external electrostatic potential at points $\mathbf{r}_j$ ($V_j = V_{el}(\mathbf{r}_j)$), and $\mathbf{A}$ is the $M \times M$ nonsingular matrix with matrix elements

$$A_{ij} = \frac{1}{|\mathbf{r}_j - \mathbf{r}_i|} \quad \text{for } j \neq i \text{ and } A_{jj} = 1.07(4\pi/S_j)^{1/2} \qquad (5)$$

Nondiagonal elements A_{ij} represent a generic Coulomb interaction between surface elements $\mathbf{r}_i$ and $\mathbf{r}_j$. The diagonal elements A_{jj} describe the self-interaction of the surface element $\mathbf{r}_j$. Formula 5 was discussed in detail by Klamt and Shüürmann,[17] and the coefficient 1.07 was fitted by these authors for better numerical accuracy.

SCREEP charges $\mathbf{q}$ should be determined once prior to their use in embedded cluster calculations. The calculation of $\mathbf{q}$ proceeds in three steps: (i) construct and discretize the SCREEP surface around a cluster; (ii) calculate Madelung potentials V_j on the surface elements; (iii) solve linear equations (3). In our implementation,[18] SCREEP surfaces S around clusters were built and discretized as "van der Waals" surfaces from atomic spheres of a fixed radius R_a using the gepol93 algorithm.[19] Madelung potentials V_j were calculated by using the Ewald summation technique. The matrix inversion algorithm has been used to solve equations (3).

In the rest of this paper we will consider several examples in order to illustrate the applicability of the SCREEP method as well as a strategy for achieving optimal accuracy. All quantum calculations have been done with our locally modified version of the Gaussian92/DFT computer program.[20]

3. Results

Test calculations revealed several points that should be borne in mind when using the SCREEP model. First, the SCREEP model can ensure a correct lattice potential only inside the surface S. If the radius R_a of atomic spheres is too small, tails of cluster wave functions may penetrate outside the surface S and be affected by an incorrect electrostatic potential. Thus, generally, the accuracy of SCREEP calculations is better for larger R_a. In most cases, R_a values of 2.5−3.0 Å give sufficiently accurate results. Second, the SCREEP potential improves significantly when a finer division of the surface S into smaller surface elements is used. In most cases, 60 elements per each atomic sphere provide a reasonable compromise between numerical accuracy and computational expense. Finally, the accuracy can be improved if ions from the environment that are close to the quantum cluster and surface S are treated explicitly without the SCREEP approximation; i.e., their potential is directly evaluated inside cluster and subtracted from the potential vector V in eq 4. The simplest way to specify the explicitly treated region of the environment is by selecting a cutoff radius R_{cut} ($R_{cut} > R_a$). Then all lattice ions in the environment lying within R_{cut} to the closest atom of the cluster are attributed to the explicit region.

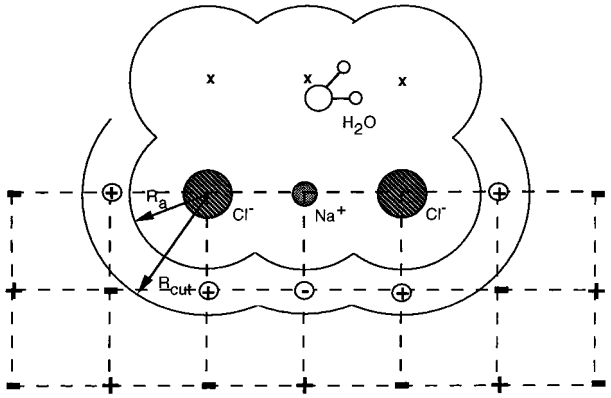

Figure 1. Side view of the $[Na_5Cl_4+H_2O]^+$ cluster on the NaCl(001) surface and sketch of the SCREEP model.

TABLE 1: Rms Deviations (in kcal/mol) from the Exact Madelung Potential above the NaCl(001) Surface for Finite Lattice Models with Dimensions $n \times n \times m$

	$n \times n$				
m	6×6	8×8	10×10	12×12	14×14
3	3.64	1.71	0.97	0.60	0.39
4	2.42	0.83	0.35	0.17	0.09
5	3.10	1.40	0.80	0.51	0.34

3.1. The Madelung Potential above the NaCl(001) Surface and Water Molecule Adsorption. In this section we consider an application of the SCREEP method to embedded cluster calculations of water adsorption on the unrelaxed rock-salt NaCl-(001) surface. We will assume for simplicity that the environment is represented by an infinite five-layer slab of point charges (± 1). To appreciate the advantages of our new approach, let us first demonstrate the performance of the traditional embedding scheme in which the infinite lattice is substituted by a neutral block with dimensions $n \times n \times m$ ($n = 6-14$, $m = 3-5$), m layers deep. Positions of ions in the block ($\mathbf{R}_i$) were the same as in the crystal lattice, and their charges were ± 1. As an indication of the accuracy, we calculated the rms deviation of the model potential $V_{model}(\mathbf{r}_j)$ from the exact Ewald potential $V_{el}(\mathbf{r}_j)$ at 21 equidistant points $\mathbf{r}_i$ having z coordinates between 1.0 and 5.0 Å directly above the surface cation. These errors are presented in Table 1. As expected, they show rather poor convergence with increasing size of the explicitly treated lattice.

Now return to the SCREEP method. The quantum cluster $[Na_5Cl_4]^+$ selected for these studies contained nine surface atoms that form a square 3×3 (the side view is shown in Figure 1). As NaCl is a rather ionic crystal, we do not expect that slight deviation from stoichiometry and assignment of the integer charge ($+1$) to this cluster will affect our results in any significant way. The surface S was constructed by making spheres of radius $R_a = 2.5$ Å around each atom in the cluster and around nine additional centers (three of them are denoted by crosses in Figure 1) having z coordinates of 4.0 Å just above each atom in the cluster. Introduction of these additional centers comes from the necessity to provide enough space for placing adsorbate molecules inside the SCREEP surface above the crystal. Each full atomic sphere was divided into 60 surface elements, so that the entire surface was divided into 442 surface elements.

The rms errors for the SCREEP potential with different values of R_{cut} are shown in Figure 2 (thin full line and squares). Even in the case where no lattice ions beyond the cluster are treated explicitly ($R_{cut} = 2.0$ Å is smaller than the interionic distance in NaCl, 2.82 Å), the error of 0.12 kcal/mol is already smaller than that for all explicit lattice models from Table 1 except for

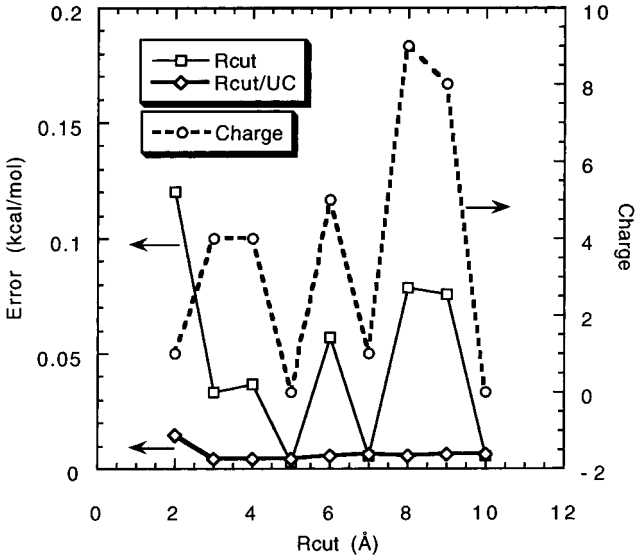

Figure 2. Results for the NaCl(001) surface. The charge of the extended cluster (dashed line) and the standard deviation of the SCREEP potential from the exact lattice potential (full lines) as functions of the cutoff radius R_{cut}.

the $14 \times 14 \times 4$ lattice consisting of 775 ions outside the cluster. For larger R_{cut} values, a more accurate SCREEP representation of the electrostatic potential is obtained, but calculated errors have some irregular dependence on R_{cut}. This behavior strongly correlates with the total charge Q_{tot} (dashed line and circles in Figure 2) of the *extended cluster* region which is defined as the quantum cluster plus the explicitly treated part of the environment. This is because for nonzero values of Q_{tot}, a significant total surface charge should be created on the surface S in order to simulate the potential from the rest of the lattice. In this case, the self-interaction of surface charges described by diagonal elements A_{jj} of the matrix **A** would have a noticeable contribution to the total potential balance on the surface. The accuracy of this term, however, is limited by the use of the empirical multiplier 1.07 in eq 5. One way to reduce this error is to select the extended cluster in such a way that its total charge is zero or small. This condition is satisfied automatically if the extended cluster is constructed from neutral unit cells. More specifically, in this modified scheme denoted as R_{cut}/UC in Figure 2, if some ion lies closer than R_{cut} to the cluster, then we attribute to the extended cluster the whole unit cell containing this ion. As seen from Figure 2 (thick full line and diamonds), such an approach, indeed, yields much better accuracy than any finite lattice model from Table 1. For example, the R_{cut} value of 3 Å leads to the error of 0.004 kcal/mol, which is not reduced by further increase of R_{cut}. In our opinion, this level of accuracy is sufficient for most chemical applications, though one can obtain even better accuracy by using a finer division of the surface S.

To illustrate the use of the SCREEP embedding method in quantum-chemical SCF calculations, we performed geometry optimizations using analytical energy gradients for a water molecule adsorbed on the quantum cluster $[Na_5Cl_4]^+$. The basis set and computational conditions were basically the same as described in our previous work.[21] Three embedding schemes were compared: no embedding at all, i.e., adsorption on the bare $[Na_5Cl_4]^+$ cluster; embedding in the finite $8 \times 8 \times 4$ lattice of point charges $q_i = \pm 1$ (247 explicit lattice ions outside the cluster); and the SCREEP embedding with $R_{cut} = 3$ Å (121 lattice ions in the explicit zone plus 422 point charges on the surface S). These results are presented in Table 2.

TABLE 2: Geometry (Distances in Å, Angles in deg)[a] and Adsorption Energy (kcal/mol) for H_2O Molecule Adsorbed on the NaCl(001) Surface Calculated Using the $[Na_5Cl_4+H_2O]^+$ Quantum Cluster and Different Embedding Schemes

	no embedding	$8 \times 8 \times 4$	SCREEP
no. of point charges	0	247	543
O_z	2.390	2.384	2.380
$O_x = O_y$	0.294	0.374	0.375
OH	0.948	0.949	0.949
HOH angle	106.4	106.2	106.2
tilt angle	19.6	5.4	5.9
adsorption energy[b]	7.5	8.3	8.3

[a] The origin was placed at the central Na^+ ion in the cluster; *x* and *y* axes were directed toward nearest surface Cl^- ions; the *z* axis pointed outside the crystal. [b] Short-range embedding effects and correlation corrections have significant effects on adsorption energy;[21] therefore, comparison with experimental data was not attempted here.

It was established in our previous studies[21] that H_2O molecularly adsorbs on the NaCl(001) surface with the oxygen atom above the Na^+ site and hydrogen atoms pointing symmetrically toward nearest anions and slightly away from the surface. As seen from Table 2, the neglect of the Madelung field in the cluster leads to some increase of the oxygen−surface distance and the molecular tilt angle (the angle between the molecular axis and the surface). This comparison may explain why recent ab initio calculations of H_2O/NaCl(001) adsorption using the Na_9Cl_9 cluster without any embedding potential[22] overestimated these parameters. The adsorption energy calculated by these authors (7.8 kcal/mol) is also close to our result for the bare cluster (7.5 kcal/mol). Results for $8 \times 8 \times 4$ and SCREEP embedding schemes agree with each other but differ from those for the bare cluster. This good agreement indicates that traditional finite lattice embedding (the $8 \times 8 \times 4$ lattice in our case) may be quite successful for simple crystal lattices if proper care is taken in selecting the finite lattice size.[5,21,23,24] Moreover, this agreement confirms our correct implementation of the SCREEP potential and corresponding energy derivatives in ab initio molecular orbital calculations.

3.2. Madelung Potential in Zeolite. In contrast to simple rock-salt structures, for many complex lattices, such as zeolites, it is not obvious how to select a finite piece of the lattice that will allow one to accurately model the crystal field. In these cases, the benefits of using our new embedding scheme versus finite lattice embedding should be especially clear. We applied the SCREEP model to the siliceous faujasite with 576 atoms in the unit cell.[25] Atoms in the environment were treated as point charges with formal values $q_O = -2.0$ and $q_{Si} = 4.0$. For a cluster we selected the molecular complex $[Si-O-Si(O)_2-O-Si]^{4+}$ located on the surface of a big channel in the faujasite structure (see Figure 3). The SCREEP surface was constructed around all cluster atoms and one additional center inside the channel. The radius of atomic spheres R_a was chosen to be 3.0 Å. The rms deviation of the SCREEP potential from the exact Madelung potential was calculated at 216 points arranged in a cubic grid $6 \times 6 \times 6$ with dimensions 2 Å × 2 Å × 2 Å located inside the channel close to the central silicon atom of the cluster. Exact Madelung potentials at these points were calculated using the Ewald method. In the first row of Table 3, we present results obtained for division of each full atomic sphere into 60 boundary elements and $R_{cut} = 3.5$ Å. The error (1.17 kcal/mol) is rather large. However, this error is already much smaller than 21.3 kcal/mol reported by Greatbanks et al.[16] or 6.3 kcal/mol reported by Cook et al.[26] The error was reduced by using a greater density of surface points (240 points/sphere) as shown in the second row of Table 3. The residual error (0.24 kcal/mol) was mainly due to the nonzero charge ($Q_{tot} = 12$) of the extended cluster. This charge effect was eliminated by explicit treatment of six more oxygen ions (charge −2) close to the explicit region, and the accuracy was further improved (the third row in Table 3). Finally, the best accuracy (the fourth row in Table 3) was achieved by increasing R_{cut} to 4.0 Å. Despite the nonzero charge of the extended cluster ($Q_{tot} = -2$), the error was reduced to only 0.05 kcal/mol. These calculations clearly demonstrate an important advantage of the SCREEP method as compared to traditional point-charge embedding schemes. Our new approach offers several simple and straightforward procedures for the systematic improvement of accuracy.

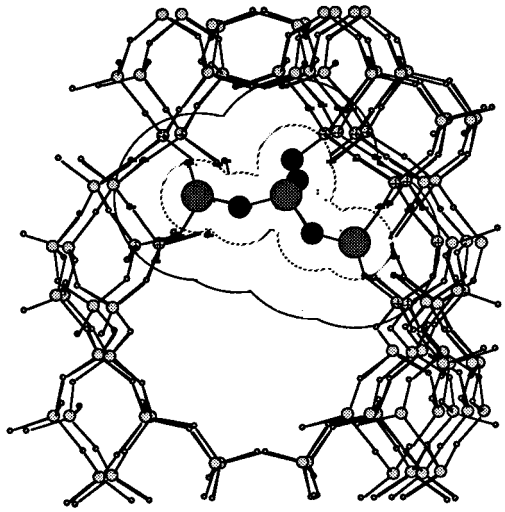

Figure 3. The cluster $[Si-O-Si(O)_2-O-Si]^{4+}$ in the faujasite structure. Larger circles denote Si atoms and smaller circles denote O atoms. The SCREEP surface (broken line) and the boundary of the explicit zone (full line) are shown schematically.

TABLE 3: Calculation Parameters and rms Deviations from the Exact Madelung Potential for the SCREEP Potential in Zeolite Calculations

	M	no. of explicit lattice charges	Q_{tot}	R_{cut}, Å	error (kcal/mol)
I	158	27	12	3.5	1.17
II	641	27	12	3.5	0.24
III	641	33	0	3.5	0.11
IV	641	40	−2	4.0	0.05

4. Discussion

It is interesting to compare the computational expense required for calculation of *matrix elements* of the crystal electrostatic field by using the SCREEP method versus the direct Ewald summation.[11] We cannot make a direct comparison because the program for calculating Ewald matrix elements is not available to us. However, we can estimate the relative performance of these two methods by comparing the time for calculation of the electrostatic *potentials*. With 641 surface charges and 40 explicit lattice charges (line IV in Table 3), the SCREEP calculation of the electrostatic potential at 216 points in a zeolite pore took only 0.5 s on an IBM RISC/6000 model 370 workstation. A total of 40.5 s was required for evaluating the Ewald series with summation indices running from −1 to +1 for both direct and reciprocal lattices. Although the SCREEP method is 2 orders of magnitude faster in this case, the Ewald summation is more accurate. Taking the convergence parameter for the Ewald method from eq 55 in ref 11, we found the rms deviation from the exact potential in 216 points of only 0.0007 kcal/mol. This should be compared with 0.05 kcal/mol

accuracy given by the SCREEP method. However, the accuracy of the potential given by SCREEP is already sufficient for quantum-chemical applications as indicated in our discussion of the H_2O/NaCl calculations from section 3.2. This suggests that further improvement of the accuracy beyond 0.05 kcal/mol is not warranted.

Another important difference between these two methods is their behavior with respect to an increase in the size of the system. The computational time for the conventional Ewald summation of matrix elements grows linearly with the number of atoms in the unit cell. However, the time required to calculate matrix elements with SCREEP charges does not depend on the size of the crystal unit cell. Therefore, SCREEP calculations should be preferred for systems with large unit cells, such as zeolites, crystal surfaces, or proteins. The number of SCREEP surface charges grows only as $N^{2/3}$, where N is the number of atoms in the quantum cluster. Thus, the SCREEP model does not limit the cluster size. Limitations due to evaluation of intracluster interactions, such as two-electron integrals, are much more severe. If needed, the performance of the SCREEP method can be further improved by using the fast multipole techniques proposed recently for solution of the quantum Coulomb problem (see, for instance, ref 27).

It should be noted that the SCREEP method allows one to represent only the electrostatic part of the total embedding potential. Other components (short-range, polarization, etc.) may also be important. For example, it is well-known that it is not possible to optimize positions of boundary atoms in the cluster without considering non-Coulomb embedding effects. Thus, in practical calculations with full geometry relaxation in embedded clusters, the SCREEP method should be combined with other embedding techniques such as pseudoatom,[28,29] localized orbitals,[30] pseudopotential,[8,31,32] or embedded density functional[5] methods which can adequately account for short-range embedding effects.

5. Conclusions

We suggest a simple method that allows one to incorporate the matrix elements of the Madelung potential in embedded cluster calculations of solids. The idea of the method is to replace the electrostatic potential from the extended charge distribution of the infinite crystal lattice by the potential from a finite number of point charges. An analogy with the conductor shielding of electrostatic fields suggests that for better performance these point charges should be located on a closed surface surrounding the quantum cluster. Then their values can be determined from a boundary condition describing a conductor in an external electrostatic field. With appropriate choice of computational parameters (the size of the explicitly treated region of the lattice, atomic radii, and division of atomic spheres into boundary elements), the SCREEP method can easily provide the rms deviation of less than 0.1 kcal/mol from the exact lattice potential. This accuracy level appears to be sufficient for most ab initio embedded cluster studies, though it can be further improved in a simple and systematic way. In H_2O/NaCl studies reported above, the SCREEP electrostatic embedding added only 1−2% of the computational time required for the bare molecule calculation.

The SCREEP method has shown great potential for studying important processes in crystals with partly ionic chemical bonds and on the surface of such crystals. In forthcoming papers we will report applications of this method for studies of adsorption and reactions at acidic centers in zeolites and on surfaces of TiO_2 and Al_2O_3 crystals which are currently underway in our laboratory. A combination of the SCREEP method with our recently developed computational model for solid−liquid interfaces[21] will be reported in a separate publication.[33] In addition, the SCREEP method seems promising for quantum-chemical studies of biological systems. For example, using this method, the electrostatic field of a protein (tens of thousands of atoms) on an active site can be represented by only several hundreds of point charges surrounding a suitable quantum cluster.

Acknowledgment. This work was supported in part by the National Science Foundation through a Young Investigator Award to T.N.T.

References and Notes

(1) Grimes, R. W., Catlow, C. R. A., Shluger, A. L., Eds. *Quantum Mechanical Cluster Calculations in Solid-State Studies*; World Scientific: Singapore, 1992.
(2) Kaplan, T. A., Mahanti, S. D., Eds. *Electronic Properties of Solids Using Cluster Methods*; Plenum: New York, 1995.
(3) Pacchioni, G., Bagus, P. S., Parmigiani, F., Eds. *Cluster Models for Surface and Bulk Phenomena*; Plenum Press: New York, 1992.
(4) Pisani, C.; Orlando, R.; Nada, R. In *Cluster Models for Surface and Bulk Phenomena*; Pacchioni, G., Bagus, P. S., Parmigiani, F., Eds.; Plenum: New York, 1992; p 515.
(5) Stefanovich, E. V.; Truong, T. N. *J. Chem. Phys.* **1996**, *104*, 2946.
(6) Kunz, A. B.; Klein, D. L. *Phys. Rev. B* **1978**, *17*, 4614.
(7) Kunz, A. B.; Vail, J. M. *Phys. Rev. B* **1988**, *38*, 1058.
(8) Shidlovskaya, E. K. *Latv. J. Phys. Tech. Sci.* **1996**, *4*, 57.
(9) Jaffe, J. E.; Hess, A. C. *J. Chem. Phys.* **1996**, *105*, 10983.
(10) Hammes-Schiffer, S.; Andersen, H. C. *J. Chem. Phys.* **1994**, *101*, 375.
(11) Saunders, V. R.; Freyria-Fava, C.; Dovesi, R.; Salasco, L.; Roetti, C. *Mol. Phys.* **1992**, *77*, 629.
(12) Allouche, A. *J. Phys. Chem.* **1996**, *100*, 1820.
(13) Allouche, A. *J. Phys. Chem.* **1996**, *100*, 17915.
(14) Ferrari, A. M.; Pacchioni, G. *J. Phys. Chem.* **1996**, *100*, 9032.
(15) Ferro, Y.; Allouche, A.; Corà, F.; Pisani, C.; Girardet, C. *Surf. Sci.* **1995**, *325*, 139.
(16) Greatbanks, S. P.; Sherwood, P.; Hillier, I. H. *J. Phys. Chem.* **1994**, *98*, 8134.
(17) Klamt, A.; Schüürmann, G. *J. Chem. Soc., Perkin Trans. 2* **1993**, 799.
(18) The SCREEP program is available from the authors upon request.
(19) Pascual-Ahuir, J. L.; Silla, E.; Tuñon, I. *J. Comput. Chem.* **1994**, *15*, 1127.
(20) Frisch, M. J.; Trucks, G. W.; Schlegel, H. B.; Gill, P. M. W.; Johnson, B. G.; Wong, M. W.; Foresman, J. B.; Robb, M. A.; Head-Gordon, M.; Replogle, E. S.; Gomperts, R.; Andres, J. L.; Raghavachari, K.; Binkley, J. S.; Gonzalez, C.; Martin, R. L.; Fox, D. J.; Defrees, D. J.; Baker, J.; Stewart, J. J. P.; Pople, J. A. *GAUSSIAN 92/DFT*; Gaussian, Inc.: Pittsburgh, PA, 1993.
(21) Stefanovich, E. V.; Truong, T. N. *J. Chem. Phys.* **1997**, *106*, 7700.
(22) Jug, K.; Geudtner, G. *Surf. Sci.* **1997**, *371*, 95.
(23) Johnson, M. A.; Stefanovich, E. V.; Truong, T. N. *J. Phys. Chem. B* **1997**, *101*, 3196.
(24) Stefanovich, E. V.; Truong, T. N. *J. Chem. Phys.* **1995**, *102*, 5071.
(25) Mortier, W. J.; Van der Bossche, E.; Uytherhoeven, J. B. *Zeolites* **1984**, *4*, 41.
(26) Cook, S. J.; Chakraborty, A. K.; Bell, A. T.; Theodorou, D. N. *J. Phys. Chem.* **1993**, *97*, 6679.
(27) Strain, M. C.; Scuseria, G. E.; Frisch, M. J. *Science* **1996**, *271*, 51.
(28) Sauer, J. *Chem. Rev.* **1989**, *89*, 199.
(29) Bredow, T.; Geudtner, G.; Jug, K. *J. Chem. Phys.* **1996**, *105*, 6395.
(30) Gorb, L. G.; Rivail, J.-L.; Thery, V.; Rinaldi, D. *Int. J. Quantum Chem.: Quantum Chem. Symp.* **1996**, *30*, 1525.
(31) Vail, J. M. *J. Phys. Chem. Solids* **1990**, *51*, 589.
(32) Puchin, V. E.; Shluger, A. L.; Tanimura, K.; Itoh, N. *Phys. Rev. B* **1993**, *47*, 6226.
(33) Stefanovich, E. V.; Truong, T. N. In *Hybrid Quantum Mechanical and Molecular Mechanical Methods*; Gao, J., Thompson, M. A., Eds.; ACS Books: Washington, DC, 1998 (in press).